LightStream – enhancements introduced to the Astrometry24.NET, photometric and astrometric software for processing SST and asteroid optical images from CCD and CMOS cameras

Agnieszka Gurgul[1], Michał Drzał[1], Agnieszka Sybilska[1], Piotr Sybilski [1], Mariusz Słonina[1], Natasza Siódmiak[1], Grzegorz Lech[1], Rafał Ślimak[1], Maciej Pilichowski[1], Adam Kinasz[1], Wieńczysław Bykowski[1]

[1] Sybilla Technologies, ul. Toruńska 59, 85-023 Bydgoszcz, Poland, agnieszka.gurgul@sybillatechnologies.com

ABSTRACT

LightStream, funded by the Polish National Center for Research and Development, is a project dedicated to the development of innovative software for efficient and accurate astrometry and photometry of point and streak sources from astronomical CCD and CMOS cameras.

In this paper we focus on the rolling shutter effect in LEO observations from one of our prototype stations PAN2 in Spain. We discuss the scale of the effect, its compensation and results for LEO as well as MEO and GEO objects for comparison. We also showcase the project's progress in the following areas: compression, stacking, plug and play, modularity, and versatility.

1 INTRODUCTION

The LightStream project responds to the needs arising from the growing number of SST objects to be observed, as well as to the technical leap in the amount and speed of data provided by optical sensors: the change from CCD to CMOS means a 100+ -fold increase in the amount of data to be processed and stored. Another motivation is the effective detection and measurement of objects with non-sidereal movement (satellites, space debris, asteroids). Currently, no off-the-shelf software is available that would allow such measurements for CCD and CMOS cameras.

LightStream provides software for astrometry and photometry of detected objects, along with a pilot environment for software testing, allowing for a significant reduction in the amount of data stored and processing time from acquisition by the sensor to onward transfer to artificial Earth satellite security services, NEO-related services that rely on optical observation stations with CCD, CMOS cameras. To ensure that the solutions are as complementary as possible, the software is tested for different angular velocities and brightness of objects, different camera parameters or modes of operation, optics used, etc.

One of the challenges the project addresses is the automatic reduction of data from CMOS cameras equipped with the electronic rolling shutter, which are becoming increasingly popular on the astronomical market. For these camera types the method for correct determination of observation epoch is different from the approach used for CMOS cameras with global shutter or CCDs.

2 LIGHTSTREAM INNOVATIONS

2.1 Compression

The data compression used in the LightStream take place on several different levels, ranging from reducing disk space consumption by thoroughly removing backgrounds from scientific images, characterizing objects within the frame and using different binning factors to the raw data. Objects' data is limited in precision to the necessary range based on the error of the measurement (1/10 or 1/100 of the error value), stellar objects are removed in baseline Space Safety case.

LightStream sensor part focuses on extraction and characterization of points and streaks present in optical data. Extracted features of non-stellar objects along with individually assigned descriptors as well as descriptors for image are uploaded to the cloud part. Features and descriptors extracted from a single observation are aggregated inside a single file which is uploaded to the cloud via protocol tailored to file transfer. File transfer is also assumed to be performed within a secure and encrypted connection as well as authenticated and authorized using industry standards OpenID Connect and OAuth 2.0.

Single file containing optical observations contains:

- Metadata describing optical measurement.
- Astrometric solution computed from stars in the field.
- Photometric solution.
- Correlation for each of the known features (stars, artificial objects, SSO).
- List of extracted point features along with their descriptors.
- List of extracted streak features along with their descriptors.

In the baseline scenario only non-stellar objects are uploaded to the cloud and stellar observations are

Proc. 2nd NEO and Debris Detection Conference, Darmstadt, Germany, 24-26 January 2023, published by the ESA Space Safety Programme Office Ed. T. Flohrer, R. Moissl, F. Schmitz (http://conference.sdo.esoc.esa.int, February 2023)

discarded on the sensor's side. The file is compressed for transfer purpose.

Selected format used for message serialization needs to provide minimal overhead in terms of size as well as good compressibility for long-term storage.

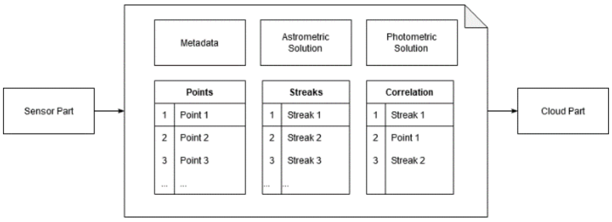

Figure 1. Overview of message with compressed frame sent from sensor to the cloud part.

2.2 Modularity

Modularity in LightStream architecture is achieved on many different levels:

- Modularity of source code
- Modularity of the architecture
- Modularity of the deployment process

LightStream aggregates and integrates plethora of complex algorithms at each stage between the data acquisition up to storing and querying compressed results. Complexity of such system necessitates dividing into smaller components which have single responsibility and properly segregated interfaces, while retaining ability to flexibly compose those components using dependency injection. For many stages (e.g. feature extraction) multiple algorithms need to be evaluated, chosen during processing and in some cases results from different algorithms need to be merged together (e.g. bright vs dark feature extraction). Interface segregation, open-closed principle ad Liskov substitution principle are crucial in this endeavor.

This is also important as basic modules of LightStream can be available in different configuration – either as standalone command line modules running on sensor premises but also as services available in cloud.

2.3 Plug and play

Plug&Play (PnP) is an important aspect of the LightStream as most of existing solutions have steep learning curves or cover only part of the process and leave the difficult integration and negotiating contracts between components coming from different providers. The complexity of such process is often discouraging proportionally to the time that is required to achieve first usable results.

Sensor part of LightStream is a software pipeline that can be both deployed on existing PC as well as delivered preinstalled with industrial PC. From user perspective plug&play of configuration manifests itself in several ways:

- Limited number of steps required for setting up environment.
- Limited number of choices required from the end-user in order to acquire satisfiable results.
- Short amount of time between receiving the product and using it.
- Clear, step-by-step procedure to follow.
- Familiarity of the configuration process.

2.4 Stacking

Stacking is performed for three distinct scenarios:

- NEO stacking – telescope tracks star field and stacks stars on top of each other
- GEO stacking – telescope points to a fixed point int the sky and gathers as much light as possible from objects while removing stars passing through the field in order to allow for stack as long as possible
- LEO stacking – telescope tracks fast moving object on the LEO orbit while removing stars passing through the field in order to allow for gathering as much light as possible

An example result for NEO stacking is shown in Figure 2 for stacking run consists of 19 exposures of 1994 PC1, 2 minutes each, stacked up to total 38 minutes of exposure.

A GEO stacking example is shown in Figure 3 - CONST stacking run consists of 10 frames 1s each observing field around 6° E.

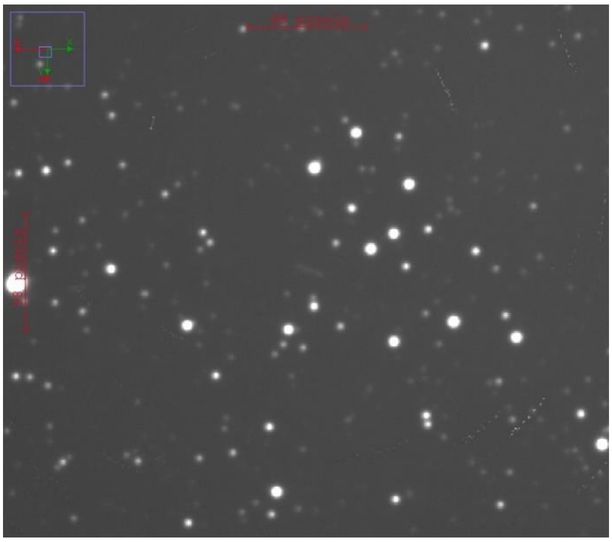

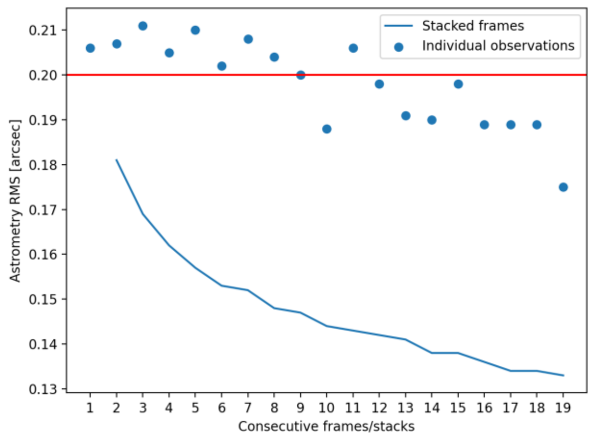

Figure 2. Top: closeup on 1994 PC1 visible a streak on image obtained with the Panoptes 4 (PAN4) sensor. Warm pixels left on frame show how much frame was rotated in order to be stacked. Bottom: Astrometric RMS – showing consistent improvement in RMS of astrometric fit over solutions from single frames. Median of frame RMSs marked with red line – each frame is a 120s exposure

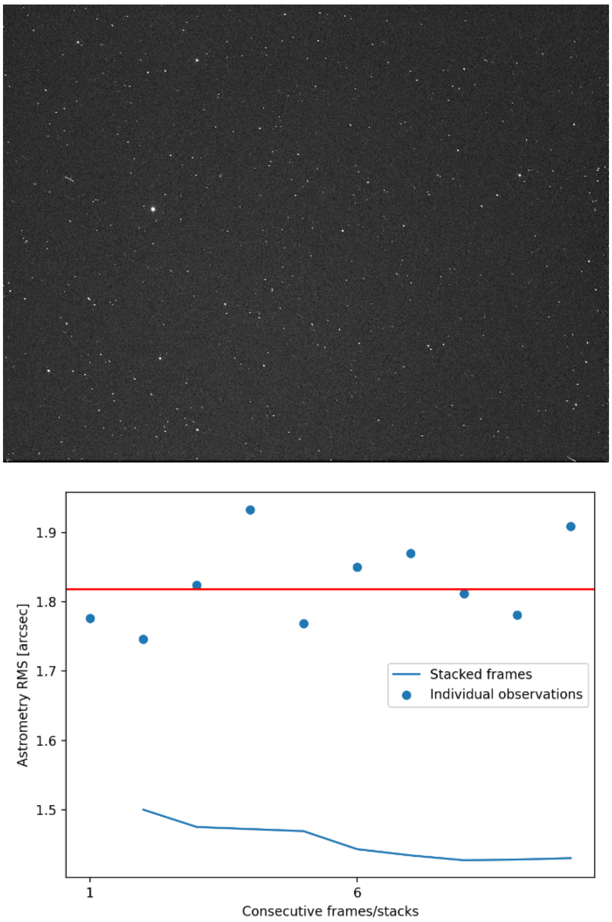

Figure 3. Top: Stack of 10 frames 1s each - total 10 s of exposure time. Bottom: stacking with star alignment reduces RMS of astrometric solution, each frame in stack has 1s exposure.

For LEO stacking similar strategy is used as with GEO with the exception of much shorter exposure times (100 ms) with total stack time up to 1.5 seconds. Stacking was performed for frames from Panoptes 9 (PAN9) sensor and COSMOS 2088 geodetic satellite.

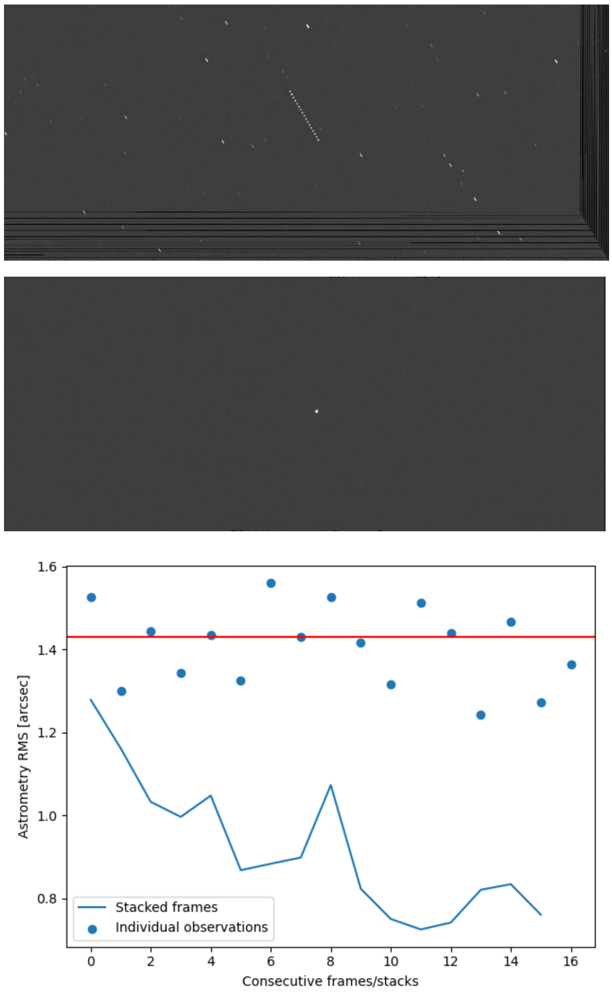

Figure 4. Top: stack of 17 frames, 0.1 s each - with total 1.7 s exposure. Middle: stack of 17 frames, 0.1 s each with star sources removed for total of 1.7 s Bottom: stacking with star alignment reduces RMS of astrometric solution, each frame in stack has 1s exposure.

2.5 Versatility

Precise characterization of optical observation is a challenge present in many distinct fields:

- Space Surveillance and Tracking (SST) of man-made objects,
- Near-Earth Objects (NEO) monitoring (natural space objects),
- astronomy (e.g. characterization of objects brightness over time using light curves),

- astrophotography.

LightStream is one tool that can be used for all of the above

Source extraction is performed initially simultaneously to pulling all required catalogue data. It is performed based on estimated background mean level and noise in each subregion of the image and objects which contain required minimum count of pixels above specified threshold. This is a standard technique used in source extraction like other software such as SEXtractor. On top of blobs extracted additional process connects sources along straight lines using probabilistic Hough transform. For sources with HFD (half-flux diameter) values diverging significantly from the median value for matched stars additional deblending procedure can be run using combination of watershed algorithm with multi-PSF fitting. Each of detected sources is then timestamped. In the case where global shutter is used in the optical sensor then a single timestamp of the middle time of the exposure is sufficient. When sensor uses rolling shutter each of the blobs has a middle time of exposure which becomes position-dependent.

2.5.1 Sidereal observations of star fields

Characterisation of stellar background is always performed as initial step of processing every frame. All blobs are extracted and characterised and matching routine is initiated which matches stars to their respective blobs. Matching can be performed against variety of catalogues:

- The Fourth US Naval Observatory CCD Astrograph Catalog (UCAC4)
- Gaia Data Release 2 (Gaia DR2)
- Yale Bright Star Catalog
- PPMXL
- The ATLAS All-Sky Stellar Reference Catalog

With default catalogue being Gaia DR2. For precise matching of stars, especially stars with large proper motions additional transformations are performed considering positional properties of catalogue entries to achieve greater astrometric precision of produced astrometry.

Additionally for each matched star aperture photometry is computed and PSF (point spread function) is fitted. Resulting characterization of each point source is persisted in final output along with matched catalogue entry.

2.5.2 Satellite observations

Since LightStream can perform both astrometry on streak and point sources it can serve both tracking satellite scenarios where tracked object is a point source and stellar background consists of streaks as well as survey scenario where stars are point sources and satellites are streaks passing the field.

All objects not associated with stars can be matched against satellites – either using information provided in observation metadata (Two-Line elements) or given time and processed frame centre computing list of satellites which should appear in the field of view. For subset of satellites there exist formats providing better precision for position and velocity. SP3 (Standard Product version 3) is used for specification of GNSS satellites and CPF (Consolidated Prediction Format) is used by satellite laser ranging stations to measure satellite positions. Both formats are supported and can be correlated against in LightStream. For each correlate satellite full information including its position and brightness info is saved to the output allowing for generation of standardized data products such as TDM (tracking data message).

2.5.3 Solar system objects

Uncorrelated objects are also compared against MPC (Minor Planet Catalog) to check for correlation with objects in orbit around Sun. LightStream periodically downloads all MPC orbits and integrates them accounting for perturbations from larger Solar System bodies. Integration is performed daily and allows for precise correlation of solar system objects including near-Earth objects. Correlated entries are persisted in processing output allowing for generation of data products.

2.5.4 Unknown objects detection

LightStream is also capable of detecting objects which are not correlated with any catalogue but instead are detected by analysis of consecutive frames where feature is persistent across the sequence. This is known as tracklet linking and allows for detection of unknown objects. Such tracklets are saved to output allowing for generation of standardized data products such as TDM and allowing further processing allowing for identification of known objects or initial orbit determination for newly discovered objects.

2.5.5 Large variety of test data

Collected observational data provides a test environment for the solutions being developed in the project. A key aspect during the selection of such a sample was to cover the greatest possible variety of data from existing optical sensors, located all around the world. Among the data collected during hundreds of observation hours are stellar targets, NEO and artificial Earth satellites, tracking and survey data, data from telescopes with mirror diameters ranging from 20cm up to 1m, with wide or narrow field of views, resulting in a diverse range of pixel scales. Optical sensors used for data gathering are equipped with the CCD or CMOS cameras from manufacturers including QHYCCD[1], FLI[2], Andor[3], Moravian Instruments[4] with nominal full resolution between 1K x 1K and 9.6K x 6.4K.

For each sensor, it was important to acquire observations of GNSS satellites used for sensor calibration. The information extracted from these measurements plays an essential role in formulating a universal approach for proper determination of the epoch of observations that arise from the technological differences between CCD , CMOS cameras with global shutter, and more commonly used CMOS cameras with electronic rolling shutter.

3 ROLLING SHUTTER EFFECT

3.1 Background

New technologies pose a number of challenges to consider when processing or analysing observational data. With greater availability, capabilities and competitive prices - relative to CCD alternatives, scientific CMOS cameras are becoming increasingly popular in the SST field, but depending on the technology used for data readout, they may require some special approaches. The use of an electronic rolling shutter on CMOS cameras makes it possible to achieve higher frames per second rates than the more expensive and less commonly used electronic global shutter.

Rolling shutter is a method of image capture where not all parts of the scene are recorded at exactly the same instant. In contrast, in global shutter entire frame is captured at the same instant. While this complicates processing of images, it allows for an increased frame rate since the exposure of an entire frame does not need to stop for the readout of a previous exposure.

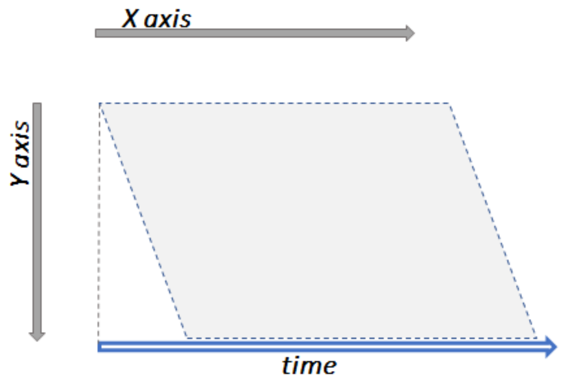

Figure 5. Time interval between the starts of exposure of each consecutive line of the frame in the rolling shutter mode is called line period.

Typically, CMOS cameras in astronomy read line by line from the first line of the frame, according to the digital line order. As a result readout for the entire frame can take longer than a single exposure so the first line of the exposure can be separated in time domain from the last line by a large time difference (see Figure 5). This time difference can be a source of image artifacts and distortions.

The main effect rolling shutter introduces is the notion that each image row effectively has its own exposure start and end and hence blobs corresponding to observed objects are observed at different times depending on where on the frame they are observed and this fact needs to be taken into account when generating timestamped tracklets as well when searching for correlation.

Some cameras also distinguish two modes of exposure - short and long - for which the limiting value is usually a single or a multiple of line period value. Part of the camera's characteristic values may change depending on the exposure mode used.

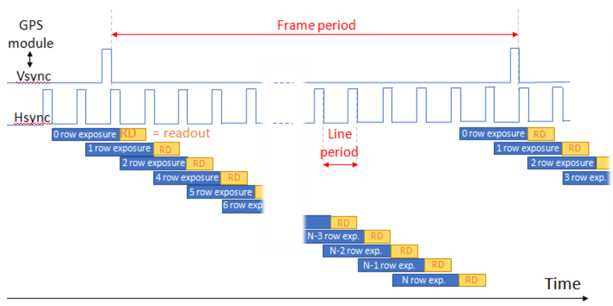

*Figure 6. Rolling shutter plot for case when exposure duration is 2*line periods.*

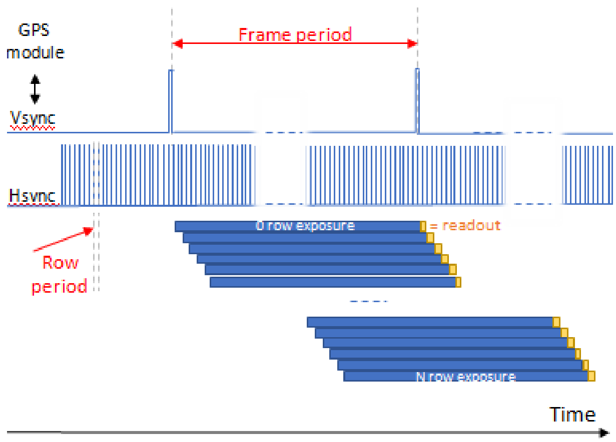

Figure 7. Rolling shutter plot for long exposure mode

Precise timing studies of the cameras electronic behaviour as well as LEO, MEO and GEO satellites observations have shown the magnitude of the rolling shutter effect on observational data. The availability of a large and versatile sample of test data collected for the

[1] www.qhyccd.com
[2] www.flicamera.com
[3] https://andor.oxinst.com
[4] https://www.gxccd.com

project allows for correlation studies between the position of the objects on image and measured astrometric position compared to the 'ground-truth' position of an object determined from SP3 or CPF ephemeris. The rolling shutter effect compensation plays a key role when analysing a series of SST observations, especially for high-resolution images, fast-moving objects or images recorded in motion.

3.2 Lab measurements

Most of the test data from CMOS cameras were taken in rolling shutter mode. Due to the differences in the beginning and end of the exposure of each row of camera data, this time delay should also be taken into account during data analysis. The difference between the beginnings of exposures of successive lines, the so-called line period, is a measurable value and is constant for a given camera, which was confirmed during testing of three of the CMOS cameras.

The precise measurements of QHY268M camera characteristics with the 6280 x 4210 SONY IMX571M sensor using oscilloscope were performed. The LinePeriod signal can be measured on the 2nd pin on the antenna cable. In order to obtain the line period value, the distance between the two electrical impulses on the oscillogram was measured (Figure 9) using different exposure parameters such as time, binning factor, the observation mode: single exposure, series of exposures or live mode. The resulting values are provided in the Table 1.

Figure 8. Back of the QHY268M camera:
1 – power supply cable, 2 – USB cable included with the camera (used to connect to a computer),
3 - antenna cable to which we connect the plug to test the pins on GPIO port (for individual signals)

Table 1. Summary of the line period oscilloscope measurements of QHY268M CMOS camera.

Binning Factor	Measured Line Period	Exposure time
1 x 1	34.7 µs	10 s
1 x 1	34.7 µs	5 s
1 x 1	34.7 µs	4 s
1 x 1	34.7 µs	3 s
1 x 1	34.7 µs	2 s
1 x 1	34.7 µs	1 s
1 x 1	34.7 µs	500 ms
1 x 1	34.7 µs	200 ms
1 x 1	34.7 µs	100 ms
1 x 1	34.6 µs	50 ms
2 x 2	34.7 µs	10 s
2 x 2	34.7 µs	5 s
2 x 2	34.7 µs	4 s
2 x 2	34.7 µs	3 s
2 x 2	34.7 µs	2 s
2 x 2	34.7 µs	1 s
2 x 2	34.7 µs	500 ms
2 x 2	34.7 µs	200 ms
2 x 2	34.7 µs	100 ms
2 x 2	34.7 µs	50 ms

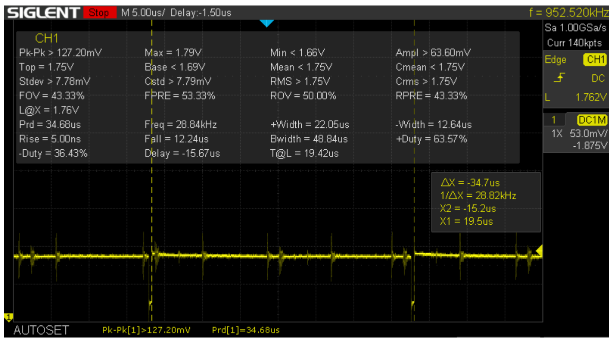

Figure 9. Oscilloscope measurements of line period from the QHY268M Pro camera. Oscilloscope used in test SIGLENT SDS1004X-E).

Presented cameras hardware allows also to retrieve information about pixel period, line period, real frame period, exposure mode etc. for each exposure.

The range of measured exposure time values for QHY268M Pro camera was 10 – 295 ms, with step 5ms and with 1ms step around expected frame period value – 34.7 µs.

The results for QHY600M Pro CMOS camera with SONY back-illuminated IMX455M sensor and rolling shutter mode used on PAN2 observations was also examined. Effective pixel area is 9600 x 6422 with overscan and optically black area. Tested exposure range covered 10 – 500 ms with 5 ms step, including 285 - 310 with step 1ms, while expected frame period value was 295.232 µs.

Table 2. Summary of the most essential in current analysis tested QHY cameras characteristics. Expected Frame Period was estimated by multiplying Line Period and frame Height in full resolution.

Camera	QHY268M Pro	QHY600M Pro
Sensor	Sony IMX571M	Sony IMX455M
Full Resolution Width	6280	9600
Full Resolution Height	4210	6422
Pixel Period [ns]	13.888	13.888
Line Period [µs]	34.666	45.972
Expected Frame Period [ms]	145.944	295.232

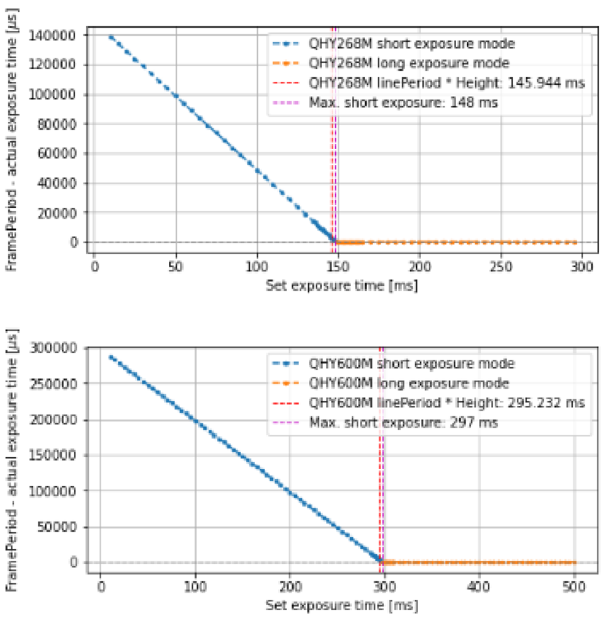

Figure 10. The difference between frame period and actual exposure time reported by the cameras from (top) QHY268M Pro and (bottom) QHY600M Pro cameras considering the distinction between short and long exposure mode.

Differences in camera behavior for short and long exposure modes were noted for all of the examined QHY cameras. Transition exposure values between these modes were determined experimentally with an accuracy of 1 ms and reproducible results were obtained. The cut-off values are several ms higher than the expected frame period. However, the key finding is that for short exposure mode frame period is much larger than the exposure time, while for long exposure mode there is no or very small difference between them, which can lead to inaccuracies in the interpretation of camera triggers, and thus timestamps, when using very short exposure times.

3.3 Test data

One of the requirements for all test data is to provide information on the precise time and location of observations, e.g., in the form of timestamps from the GPS module for each exposure with assumption of max. 1 ms accuracy. To avoid inaccuracies in the GPS module's communication with the camera, observed when using short exposure modes, all analyzed data were taken with exposure times greater than the estimated frame period.

The faster the observed object moves, the greater the potential influence of the rolling shutter effect on the measurements. For this reason, a sample of data for objects in different orbital altitudes were analyzed.

The test data were obtained using the prototype sensor Panoptes 2 (PAN2) located in Spain equipped with the QHY600M Pro camera with electronic rolling shutter. Observations were made in object tracking mode, with software binning 2x2 without subframing. In addition, when tracking a LEO object, a fixed time offset was introduced to the mount clock to cause a more visible shift of the object's position on the frames in the series.

The LEO observations of AJISAI #16908 satellite, selected sample from operational GNSS satellites of Galileo constellation and measurements of a few GEO targets are presented. For AJISAI the average angular velocity in orbit is over 186 arcsec/sec, while for Galileo satellites average is 25.6 arcsec/sec and for GEO 15.0

arcsec/sec[5].

For LEO and selected MEO satellite the CPF orbit prediction files from DGFI-TUM[6] were used for reference, while for GNSS MEO satellites the SP3 ephemeris obtained from ESA Navigation Support Office[7] resources. However due to possible variations in the accuracy of the CPF data, the values used are given only for the purpose of comparing relative values. For sensor and observational data calibration, only the SP3 FINALS files were used as reference data. The only ephemeris available for vast majority of GEO satellites is the TLE which is associated with its epoch and thus can quickly become outdated so it cannot be used for calibration. Modules responsible for artificial satellites correlation in Astrometry24.Net uses TLE in order to identify the object and filter outliers during tracklet building.

3.4 Results

The correction applied to the epochs of observations obtained by minimizing the CPF correlation residues for AJISAI satellite is consistent with the theoretical calculation of the rolling correction value resulting from the change in the position of the object on successive observation frames as shown in Y vs. X plot (Figure 11 and Figure 12).

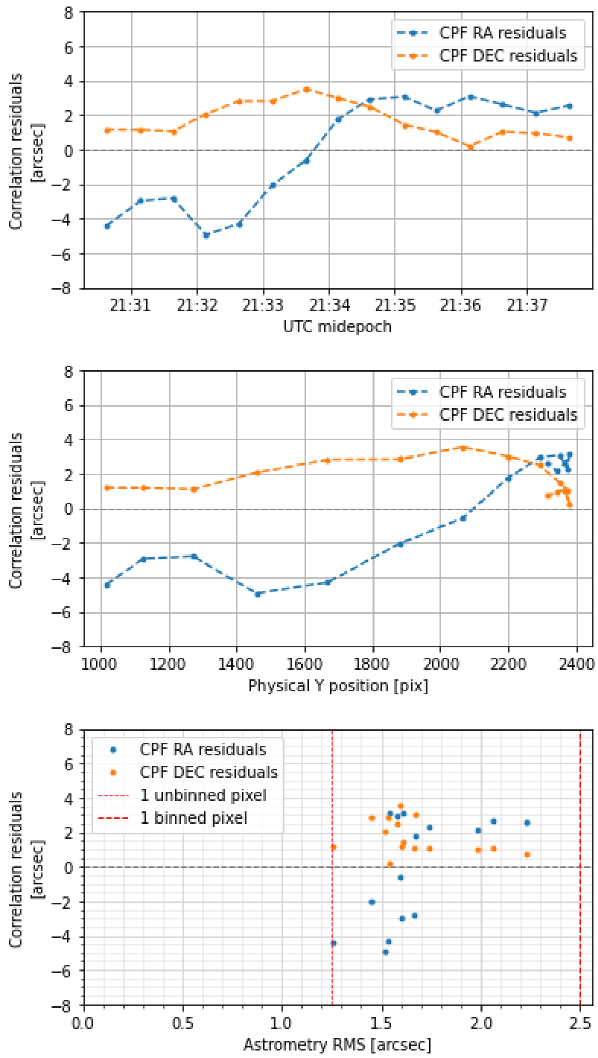

Figure 11. Minimized correlation residues of a LEO satellite AJISAI #16908 obtained with the PAN2 sensor in July 2022 in binning 2x2 with effective pixel scale of 2.5 arcsec/pix. The reference position of the satellite was obtained based on CPF file.

The linear dependency of time correction applied to the observation epochs and Y-axis position presented in Figure 13 allows to calculate that 1 ms corresponds to 10.441 pixels so a change of 1 row will be 95.77µs and after taking into account binning this translates into 47.89 µs difference between neighbouring rows. Due to the size of the object in the images, and then the accuracy of determining the centroid coordinates of the satellite, the binning, pixel scale as well as the precision of the astrometric model, the values obtained are subject to certain measurement uncertainties, whose discussion

[5] Average angular velocities were determined based on the latest TLEs obtained from www.space-track.com as of 19/01/2023.

[6] Deutsches Geodaetisches Forschungsinstitut der Technischen Universitaet Muenchen (DGFI-TUM) https://edc.dgfi.tum.de/en/data/cpf/

[7] *http://navigation-office.esa.int/GNSS_based_products.html*

goes beyond the scope of this paper. However, the compliance of the result up to 2 µs with the 45.97 µs line period value reported by the camera we consider a success.

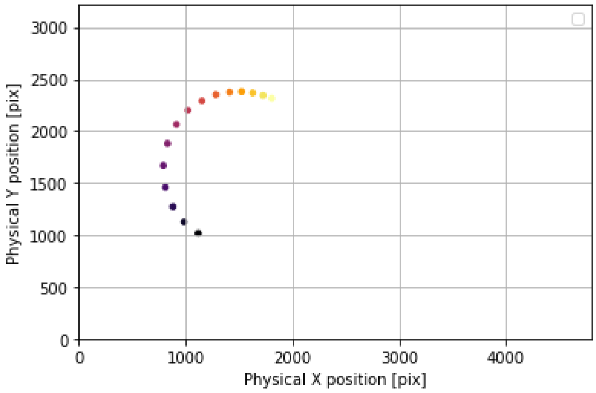

Figure 12. Shift in physical coordinates of the AJISAI satellite in analyzed FITS frames.

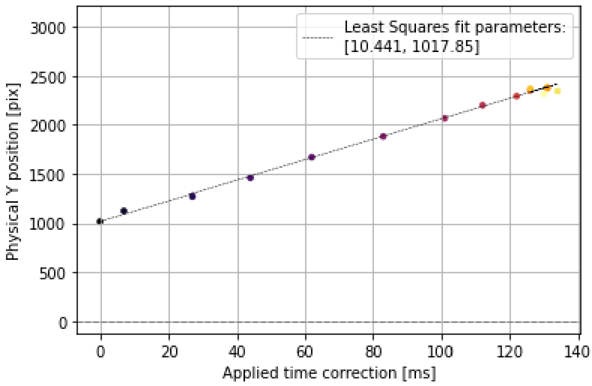

Figure 13. Relation between the object Y-position and applied time correction for AJISAI satellite. To limit the influence of CPF ephemeris accuracy used to minimize residues, the time correction values were normalized to a minimum value and thus represent only an increment.

Observations of GNSS satellites from European Galileo constellation are used for sensor calibration and to determine the time bias correction value. The measured object coordinates from series of observations are compared to the reference positions from precise SP3 ephemeris. In the next step, such time interval is fitted for which the residues are minimized. For the cameras with rolling shutter time bias is incorporated with the single or multiple of neighbouring lines, in contrast to the cameras with global shutter, when the determined value of time bias is the same regardless of the position of the object on the frame. For this reason a separate time bias value was determined for the average Y-axis position of each Galileo satellite in presented sample.

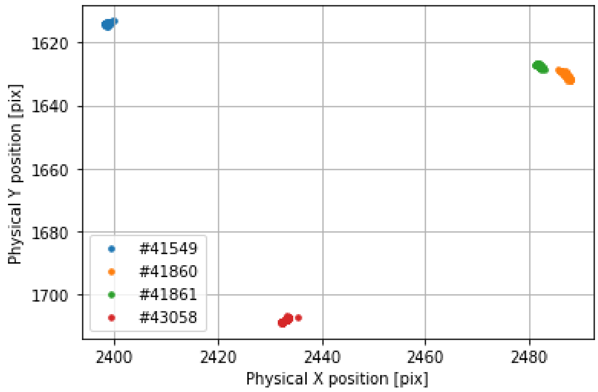

Figure 14. Physical coordinates of the selected Galileo satellites observations form PAN2. All used data comes from observing nights 2-9 of June 2022.

Table 3. Summary of time bias fitting results for selected Galileo satellites.

Norad ID	Fitted Time Bias [ms]	Average Y position [pix]	Max. Difference in Y position [pix]
#41549	147.341	1613.949	1.72
#41860	159.751	1659.17	1.19
#41861	150.443	1627.511	1.87
#43058	154.915	1708.043	2.16

Centroid locations of analyzed calibration satellites on the images were within a several lines of pixels, which, based on the estimated line period duration, can be assumed to be below 1 ms and, due to its very small value, is not possible to distinguish in measurements.

The estimated time bias correction for satellites located i.e. in the center of the field of view partially compensate the rolling shutter effect, which is a consequence of a time differences between the first camera lines for which, in case of this camera timestamps from GPS module are related for, and the middle lines with the object. To obtain time bias referring to the first image rows instead of the center, this time difference must be subtracted.

Maximum difference between satellites Y position is around 94 pixels, while the difference of the determined time bias is 7.574 ms (see Table 3). This corresponds to the increase of a level of 80.49 µs for each line, and taking into account the binning factor it is 40.24 µs. The resulting estimated line period value is subject to large uncertainties due to the relatively small difference of extremely distant objects, however, it is similar order to the previously measured 45.9 µs.

The GEO observational data presented below shows an example of the application of corrections needed to properly build tracklets for multiple objects from a series of frames. For each satellite placed in different lines of the frame the corresponding value of correction was estimated and applied (see Table 4) to the raw mid-epoch calculated in the same way. At this step the obtained in GNSS analysis proper time bias correction[8] need to be applied in order to calibrate measurements epochs. Finally, the procedure need to be repeated for all frames in series and then perform residues analysis and outlier filtering based on the reference coordinates from TLE, for each object separately.

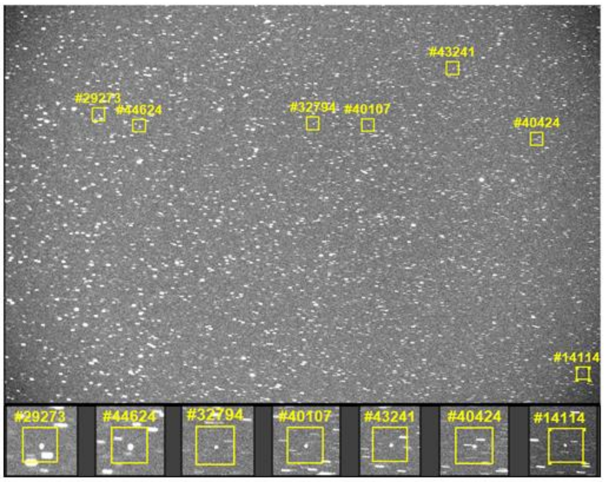

Figure 15. Sample GEO observations FITS frame from PAN2 with 4.0s exposure time in binning 2x2.Detailed information about each satellite position in the frame is presented in Table 4. The (0,0) coordinates are in top left corner.

Difference in epoch for the #43241 and #14114 object located on the same frame is around 225 ms, while their centroids are separated from each other by over 2447 rows.

The maximum difference in object position resulting from not including the rolling shutter effect in the measurement data will be equal to the frame period multiplied by the average angular velocity on GEO orbit, which would correspond to measurements of two objects located on the first and last rows of the frame, which, using the same assumptions as for the observations, would be around 4.44 arcseconds which is equal to 1.78 effective pixel of PAN2 sensor.

4 SUMMARY AND CONCLUSIONS

LightStream is intended as a fully functional (i.e. TRL 8) software suite dedicated to astronomical optical data handling. Among other aspects:

- it introduces lossy compression to significantly reduce the amount of stored data) - thus removing the need for online transfers of huge amount of raw data,
- it implements synthetic tracking to improve signal-to-noise ratio of non-sidereal moving objects, making it possible to detect objects otherwise too faint to be found,
- it puts emphasis on the ease of installation, with the goal being that the entire system can be unpacked, configured and start producing data in less than three hours.

The project also addresses the challenge of precise time measurements for the cameras with electronic rolling shutter force the need to calculate the center of exposure time for each line separately and then to link it to the object located on a given line. The use of software binning causes necessities of multiplying line period value by the binning factor to estimate the proper center epoch of exposure for each line. Using subframing, especially made in software, require the exact information about which lines were used and subtract the time that the camera spent on reading the lines not included in the final frame.

In the case of using binning and objects that usually cover an area larger than one line, the centroid coordinates of the extracted object is taken into account. As the difference between the exposure centers of successive lines are equal to line period, as for the tested cameras, where their values are in the range of 34 - 45 µs, only a shift of 20 or more lines will cause a difference in time on the level of 1 ms. This can be considered a good solution and approximation for object-related epoch of observation estimation.

For fast moving objects like on LEO or when the object is changing its position between the frames regardless its orbital altitude the rolling shutter correction application plays an important role in proper tracklet compilation.

To sum up, having the camera characteristic values and observations metadata the rolling shutter correction value can be estimated and applied automatically to the data using the LighStream software suite. Real observational data show agreement with the values obtained with oscilloscope measurements as well as the values received from the camera.

The LightStream project is scheduled for finalization in the second quarter of 2023, when the software suite will be deployed to the first client. Possible future work in the context of the rolling shutter effect includes examining

[8] By proper time bias correction author emphasizes that the time bias value for rolling shutter cameras is assigned to a specific line, and for GEO observations the same convention that was used for GNSS objects should be used.

the dependence of the applied rolling shutter correction on the position of the object along the X axis which could be an important addition to the current approach especially for high-resolution CMOS cameras.

5 ACKNOWLEDGEMENTS

The paper shows the results of the project no. POIR.01.01.01-00-0831/19-00 "LightStream - preparation and implementation for production of innovative software for efficient, accurate astrometry and photometry of point and streak sources for astronomical CCD, CMOS cameras" - project co-financed by the European Union from the European Regional Development Fund under the Intelligent Development Operational Program. The project is carried out as part of the competition of the Polish National Center for Research and Development: "Fast Path: Space Technologies".

6 REFERENCES

1. Sybilska A., Kozłowski S., Sybilski P., Pawłaszek R., Słonina M., Gurgul A., Konorski P., Drzał M., Hus S., Lech G., Litwicki M., Pilichowski M., Ślimak R., Kolb U., Burwitz V., Flohrer T., Funke Q. (2019). Astrometry24.NET – precise astrometry for SST and NEO. *In Proc. 1st. ESA NEO and Debris Detection Conference (Ed. T. Flohrer, R. John, F. Schmitz)*, ESA Space Safety Programme Office, Darmstadt, Germany.

2. Bertin E., Arnouts S., (1996) „SExtractor Software for source extraction," tom 117, pp. 393-404.

3. Gaia Collaboration et al. (2016) The Gaia mission. A&A 595, pp. A1.

4. Gaia Collaboration, A. G. A. Brown, A. Vallenari, T. Prusti, J. H. J. de Bruijne, C. Babusiaux and C. A. L. Bailer-Jones et al. (2018b) *Gaia Data Release 2. Summary of the contents and survey properties*. A&A 616 pp.A1

5. Kiryati N., Eldar T., Bruckstein A.M., (1991) *A probabilistic Hough transform*, Pattern Recognition, Volume 24, Issue 4, pp. 303-316

6. Zacharias N., Finch C.T., Girard T.M., Henden A., Bartlett J.L., Monet D.G., Zacharias M. I. (2013), *The Fourth US Naval Observatory CCD Astrograph Catalog (UCAC4)*, American Astronomical Society, Volume 145, Issue 2 pp. 44

7. Tonry J.L., Tonry, J. L., Denneau, L., Flewelling, H., Heinze, A.N., Onken, C. A., Smartt, S. J., Stalder, B., Weiland, H. J., Wolf, C. (2018), *The ATLAS All-Sky Stellar Reference Catalog*, The Astrophysical Journal, Volume 867, Issue 2, article id. 105, pp.16

8. Roeser S., Demleitner M., Schilbach E. (2010), *The PPMXL catalog of positions and proper motions on the ICRS. Combining USNO-B1.0 and 2MASS*, American Astronomical Society, Volume 139, Issue 6 pp. 2440-2447

9. Hoffleit D. , Warren Jr W.H., (1991), *The Bright Star Catalogue, 5th Revised Ed. (Preliminary Version)*, Originally published: New Haven, Conn.: Yale University Observatory, 1964, 3rd rev.ed., ed. Hoffleit, Dorrit

Table 4. Summary of the GEO satellites marked in Figure 15. Mid-epoch of this observation 2022-07-07T01:33:00.686171+00:00 was estimated as a center moment between the GPSSTART and GPSEND timestamps from FITS header. In this case, it was assumed to be the center of exposure specific to the first line of the frame. The value of the correction was calculated by multiplying the line period value, binning factor and the difference of the line indexes along the Y axis (the convention was adopted that the first line index Y_0 is 0, so the difference Y-Y_0 is Y). Due to the sub-pixel coordinates precision used in A24N, the decimal parts of the Y values were included in the calculations in order to compensate as much as possible large pixel scale[9].

Satellite NORAD ID	X [pix]	Y [pix]	Rolling shutter correction [ms]	Mid-epoch of observation with applied correction
44624	1096.0	973.5	89.507	2022-07-07T01:33:00.775678+00:00
43241	3616.5	510.2	46.910	2022-07-07T01:33:00.733081+00:00
40107	2934.6	965.8	88.800	2022-07-07T01:33:00.774971+00:00
32794	2493.5	952.8	87.604	2022-07-07T01:33:00.773777+00:00
25000	2787.1	1618.8	148.839	2022-07-07T01:33:00.835010+00:00
14114	4659.0	2958.0	271.970	2022-07-07T01:33:00.958141+00:00
29273	767.7	882.3	81.122	2022-07-07T01:33:00.767293+00:00
40424	4292.0	1080.0	99.300	2022-07-07T01:33:00.785471+00:00

[9] It should be noted that the maximum difference caused by including decimals in calculations is equal: line period*binning factor, which in this case is below 0.1ms. For optical observations, such a value has little impact on the final measurements.